Investigation of Wire Diameter of Helical Compression Spring for Payload Separation

Shandi Prio Laksono

Rocket Technology Center, National Institute of Aeronautics and Space (LAPAN), Indonesia

e-mail: shandi.prio@lapan.go.id

Received: 26-11-2020. Accepted: 07-04-2021. Published: 30-06-2021

Abstract

The payload is designed to be separated from the rocket at certain altitude. One of the critical component in the payload separation system is the helical compression spring. The helical compression spring ensures safe release of the payload. The spring must satisfy some parameters such as static failure and buckling, also spring has enough energy storing to release the payload during launch. The objective of this paper is to do investigation of wire diameter of helical compression spring which can be used in the payload separation system of sounding rocket based on several constraints. The results obtained show that with payload weight of 60 kg, minimum wire diameter should be 8 mm with mean coil diameter of 80 mm. The maximum separation velocity of 1.76 m/s was obtained by using wire diameter of 8 mm and mean coil diameter of 96 mm.

Keywords: *payload; spring; separation, diameter, rocket.*

Nomenclature

d	=	wire diameter, mm
D_o	=	outside diameter, mm
D_i	=	inside diameter, mm
D	=	mean coil diameter, mm
L_f	=	free length, m
L_s	=	solid length, m
k	=	spring rate, N/m
δ	=	deflection, m
G	=	shear modulus of the material, GPa
N_a	=	number of active coils

1. Introduction

Space launch vehicle and sounding rocket are used to place a satellite into orbit or payload in the upper atmosphere to gather scientific data. The Launch vehicle or sounding rocket places a satellite or payload into orbit or upper atmosphere by using a separation system to release it.

The separation system is a critical point for launching a satellite or payload (Hu et al., 2008). A reliable separation system ensuring the separation is free of collision and minimizing disturbance to the payload or satellite (Li et al., 2014). The launch failures of Atlas Centaur in 1970 and Chinese Long March in 1992. Also, improper in release of Titan's satellite in 1990, Pegasus in 1991 and Delta-2 in 1995 are examples of the failure of separation system (Samani, M., & Pourtakdoust, 2014).

As shown in the figure 1-1, the payload is placed in the forward end of the rocket or launch vehicle. The nose cone or fairing section is commonly used to protect the payload from aerodynamics force (Liu, Y., Li, Z., Sun, Q., Fan, X., & Wang, 2012). The payload is separated from the rocket at an altitude over 100 km (Hu et al., 2008).

ISAS (The Institute of Space and Astronautical Science) of JAXA (Japan Aerospace Exploration Agency) is operating three kinds of the sounding rockets which are S-310, S-520, and SS-520. The smallest rocket, S-310 is able to reach up to 200 km with a maximum payload weight of 50 kg (Abe et al., 2009). The SS-520 sounding rocket has a capability for launching a payload weight of 140 kg to an altitude of 800 km (Inatani, Y., Ishii, N., Nonaka, S., & Abe, 2016).

Separation system has two main functions. The first is to rigidly hold payload or satellite and rocket or launch vehicle together. The second is to influence separation of payload or satellite upon command from rocket or launch vehicle (Tayefi & Ebrahimi, 2009). Separation systems typically consist of the helical compression spring (Hu, X., Chen, X., Tuo, Z., & Zhang, 2012). The spring with length of 180 mm was capable for separating Cubesat of 1 kg at the separation velocity of 1.8 m/s (Kolawole et al., 2018).

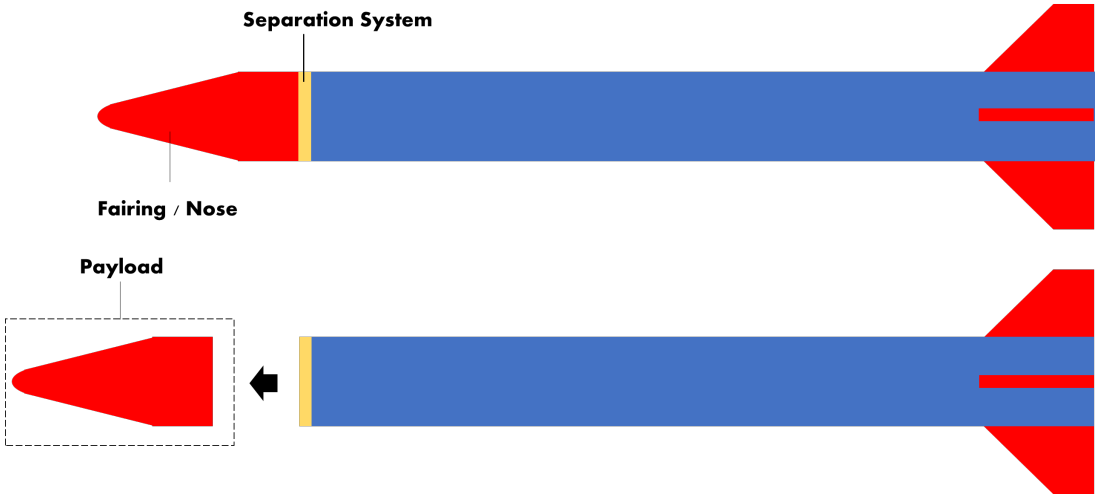

Figure 1-1: Payload Separation

2. Methodology

The objective of this research is to do investigation of wire diameter of helical compression spring which can be used for payload separation system based on several constraints. In the separation system, as shown in the figure 2-1 helical compression spring is subjected to axial load due to payload weight and deflected to its solid length. When the payload needs to be separated during flight, the release mechanism decouples the payload from the rocket and spring exert force to the payload. The spring needs to be able to withstand the payload weight without any failure.

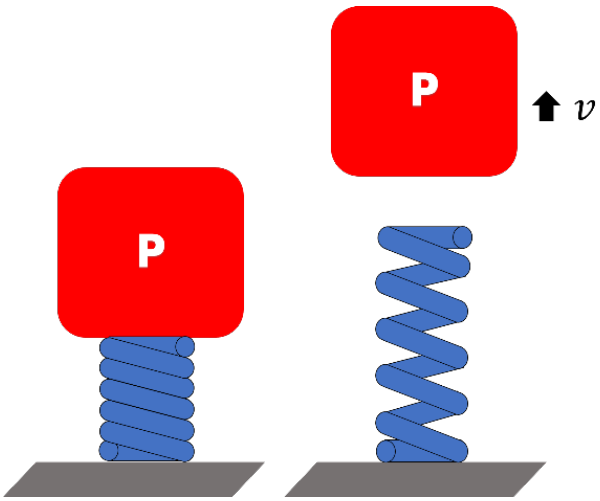

Figure 2-1: Payload and Spring.

2.1. Helical Compression Spring

A Helical compression spring is a spring with an open-coil configuration that resistance to compressive force. They have capability for energy absorption and easy to use. They usually used in machinery or equipment for controlling vibration, reducing forces due to shock loading, applying forces to members, and storing energy (Sawanobori, T., Akiyama, Y., Tsukaharat, T., & Nakamura, 1985).

A Helical compression spring is typically made from round wire, wrapped into a straight-cylindrical shape with a constant pitch between adjacent coils. Square or rectangular wire may also be used. Without an applied load, the spring's length is called the free length. When a compression force is applied, the coils are become more closely together until touch each other, at that time the length the minimum possible is called the solid length (Pattar, S., Sanjay, S.J., & Math, 2014). Figure 2-2 shows a dimensional parameter of round-wire helical compression spring.

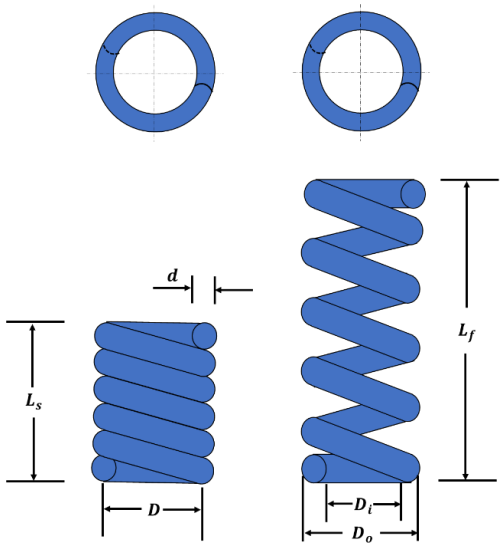

Figure 2-2: Dimensional Parameter of Helical Compression Spring.

Manufacturing of helical springs need determination of the spring parameters such as the mean coil diameter D, wire diameter d and spring index C. Other parameters such as the total number of coils N_a, free length L_f, also important design parameters to be considered (Kolawole et al., 2018). Spring index is the ratio of the mean diameter of the coil to the diameter of the wire as expressed by equation below:

$$C = \frac{D}{d} \tag{2-1}$$

Spring rate (stiffness) is the load required per unit deflection of the spring as expressed by equation below:

$$k = \frac{F}{\delta} = \frac{d^4 G}{8\, D^3 N_a} \tag{2-2}$$

$$\delta = \frac{8FD^3 N_a}{d^4 G} \tag{2-3}$$

2.2. Stress in Helical Compression Spring

The major stresses produced in helical springs are shear stresses due to twisting (Chary & Reddy, 2016). As shown in the figure 2-3, round-wire helical compression spring, loaded by the axial force.

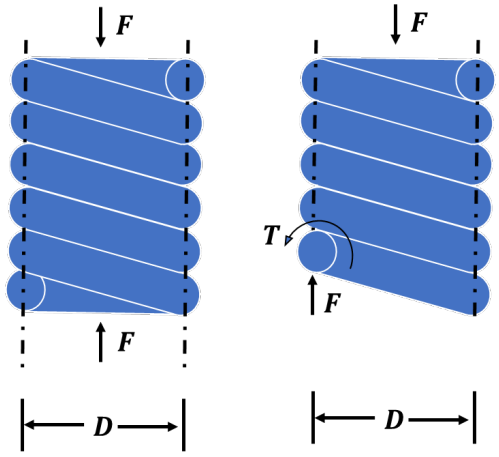

Figure 2-3: Free Body Diagram of Helical Compression Spring Axially Loaded.

The maximum stress in the wire may be calculated by superposition of the torsional shear stress $\tau_1$and direct shear stress τ_2 given by the equation below.

$$\tau_{max} = \tau_1 + \tau_2 \tag{2-4}$$

the torsional shear stress in a bar subjected to a twisting moment T is given by the equation below:

$$\tau_1 = \frac{Tr}{J} \tag{2-5}$$

where

$$J = \frac{\pi d^4}{32} \tag{2-6}$$

and

$$r = \frac{d}{2} \tag{2-7}$$

by substituting equation$(2-6)$ and $(2-7)$ into $(2-5)$, we obtain:

$$\tau_1 = \frac{8FD}{\pi d^3} \tag{2-8}$$

direct shear stress is given by the equation below:

$$\tau_2 = \frac{F}{A} \tag{2-9}$$

where

$$A = \frac{\pi d^2}{4} \tag{2-10}$$

substituting equation $(2-10)$ into $(2-9)$, we obtain:

$$\tau_2 = \frac{4F}{\pi d^2} \tag{2-11}$$

substituting equation $(2-8)$ and $(2-11)$ into $(2-4)$, we obtain:

$$\tau_{max} = \frac{8FD}{\pi d^3} + \frac{4F}{\pi d^2} \tag{2-12}$$

substituting equation$(2-1)$ into $(2-12)$, we obtain:

$$\tau_{max} = \frac{8FD}{\pi d^3}\left(1 + \frac{0.5}{C}\right) \tag{2-13}$$

then the maximum shear stress is given by the equation below:

$$\tau_{max} = K_s \frac{8FD}{\pi d^3} \tag{2-14}$$

where K_s a shear-stress correction factor and is defined by the equation below:

$$K_s = 1 + \frac{0.5}{C} \tag{2-15}$$

The ultimate tensile strength is given by the equation below:

$$S_{ut} \cong Ad^b \tag{2-16}$$

where

$$A = 1753{,}3\ MPa$$

$$b = -0.182$$

The yield shear strength is given by the equation below:

$$S_{sy} = 0.577\ (0.75)\ S_{ut} \tag{2-17}$$

2.3. Buckling in Helical Compression Spring

Buckling of steel helical compression spring with steel material and squared and ground ends is given by the equation below:

$$L_f < 2.63 \frac{D}{\alpha} \tag{2-18}$$

where α is a constant related to end condition and α values for end conditions can be seen in the table 2-1.

Table 2-1: End Condition Constants (Budynas, R.G., Nisbett, J.K, & Shigley, 2008)

End Condition	α
Spring supported between flat parallel surfaces (fixed ends)	0.5
One end supported by flat surface perpendicular to spring axis (fixed); other end pivoted (hinged)	0.707
Both ends pivoted (hinged)	1
One end clamped; other end free	2

MATLAB software was used to calculate some parameters such as maximum shear stress, yield shear strength, spring rate, deflection, free length, energy storing, and separation velocity. Calculation of the helical compression spring parameters are constrained by the following conditions:

- Payload weight: 60 kg
- Number of springs used: 1
- Cross-section of wire: round
- Solid length of spring: 200 mm
- Material of spring: Hard drawn-wire (ASTM A227)
- Shear modulus of spring: 80 GPa
- Mean Diameter of Coil: 80 ≤ D ≤ 100 mm
- Type of ends: squared and grounds

Figure 2-4 shows the flowchart of this research.

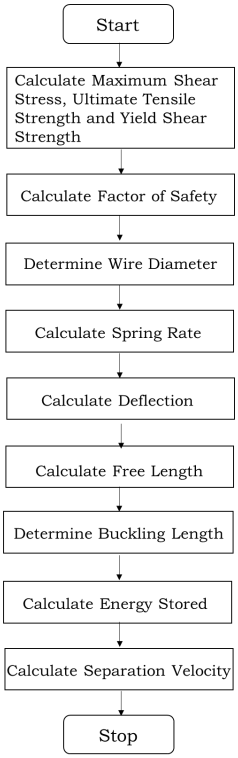

Figure 2-4: Flowchart of research

3. Result and Analysis

Figure 3-1 shows the relationship between wire diameter and maximum shear stress with mean coil diameter of 80, 90, and 100 mm. As shown in the figure, shear stress decreased with increase in wire diameter. The combination between wire diameter of 5 mm with mean coil diameter of 80, 90 and 100 mm resulted in maximum shear stress of 1,008 MPa, 1,131 MPa and 1,253 MPa, respectively. Meanwhile, the ultimate tensile strength and yield shear strength of wire diameter of 5 mm were 1,313 and 568.3 MPa, respectively. In addition, the combination between wire diameter of 10 mm with mean coil diameter of 80, 90 and 100 mm resulted in maximum shear stress of 129.9 MPa, 145.1 MPa and 160.4 MPa, respectively. Meanwhile, the ultimate tensile strength and yield shear strength of wire diameter of 10 mm were 1,151 MPa and 498.2 MPa, respectively.

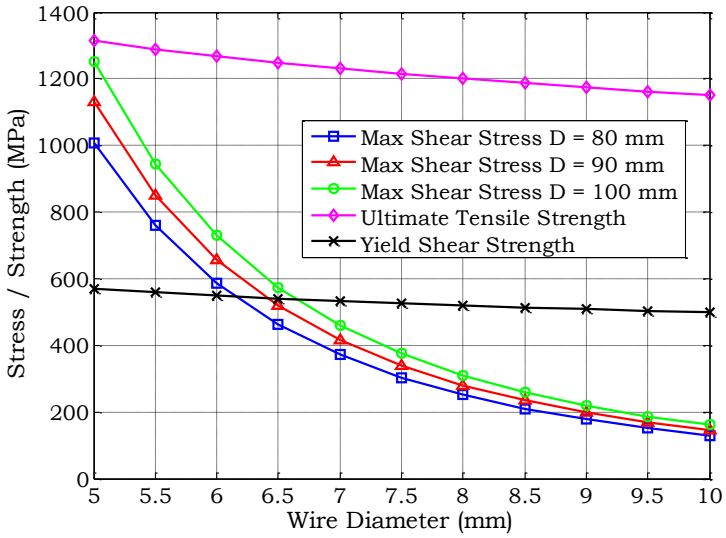

Figure 3-1: Wire Diameter vs Maximum Shear Stress.

Figure 3-2 shows the relationship between wire diameter and safety factor. As shown in the figure, safety factor increased with increase in wire diameter. Also, smaller mean coil diameter has higher safety factor. The wire diameter of 7 mm in all range of mean coil diameter 80, 90 and 100 mm has safety factor higher than 1. It means that yield shear strength of wire diameter of 7 mm is higher than its maximum shear stress. Based on these results, we considered wire diameter of 7 mm, 8 mm and 9 mm as diameter which examined to be used in payload separation system.

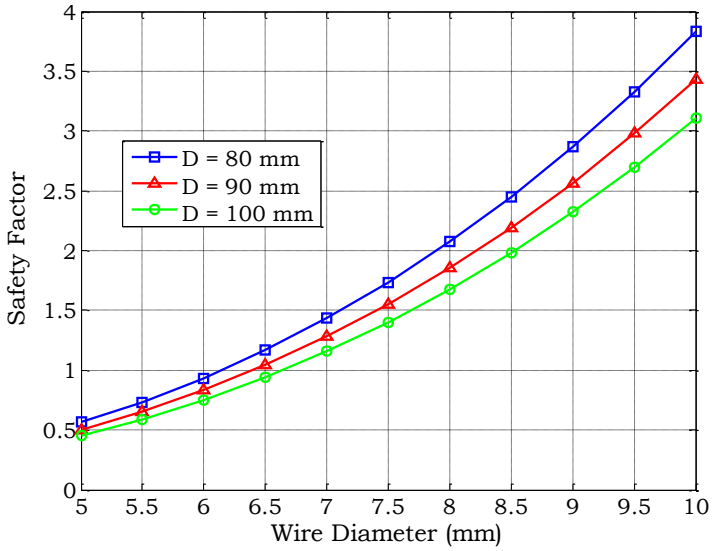

Figure 3-2: Wire Diameter vs Safety Factor.

Figure 3-3 shows the relationship between mean coil diameter and spring rate. As shown in the figure, spring rate decreased with increase in mean coil diameter. The combination between wire diameter of 7 mm with mean coil diameter of 80 and 100 mm, resulted in spring rate of 1,737 N/m and 889.3 N/m, respectively. Meanwhile, the combination between wire diameter of 8 mm with mean coil diameter of 80 and 100 mm, resulted in the spring rate of 3,478 N/m and 1,781 N/m, respectively. In addition, the combination between wire diameter of 9 mm with mean coil diameter of 80 and 100 mm, resulted in spring rate of 6,407 N/m and 3,281 N/m, respectively.

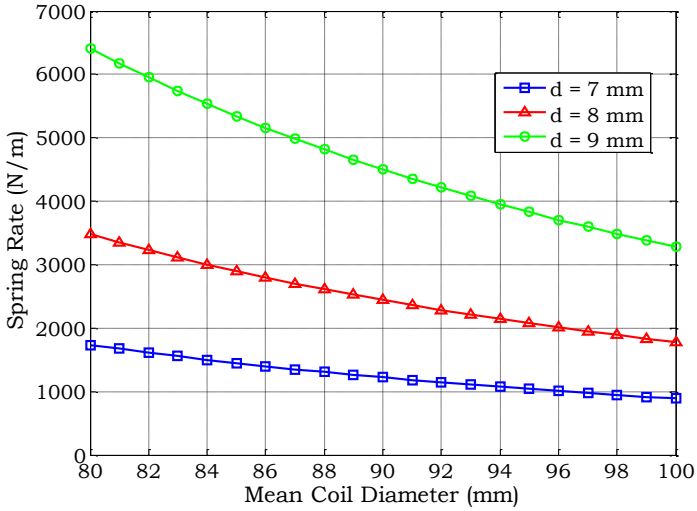

Figure 3-3: Mean Coil Diameter vs Spring Rate.

Figure 3-4 shows the relationship between mean coil diameter and deflection. As shown in the figure, deflection increased with increase in mean coil diameter. The deflection of 0.346 m was obtained by using wire diameter of 7 mm and mean coil diameter of 80 mm. Meanwhile, the combination between wire diameter of 8 mm and 9 mm with mean coil diameter of 80 mm, resulted in deflection of 0.173 m and 0.094 m, respectively.

In addition, the deflection of 0.675 m was obtained by using wire diameter of 7 mm and mean coil diameter of 100 mm. Meanwhile, the combination between wire diameter of 8 mm and 9 mm with mean coil diameter of 100 mm, resulted in deflection of 0.337 m and 0.183 m, respectively.

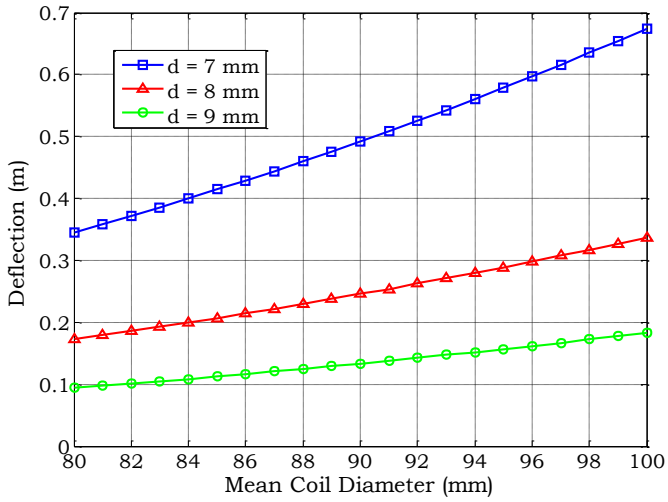

Figure 3-4: Mean Coil Diameter vs Deflection.

Figure 3-5 shows the relationship between mean coil diameter and free length. As shown in the figure, free length increased with increase in mean coil diameter. The free length of 0.546 m was obtained by using wire diameter of 7 mm and mean coil diameter of 80 mm. Meanwhile, the combination between wire diameter of 8 mm and 9 mm with mean coil diameter of 80 mm resulted in free length of 0.373 m and 0.294 m, respectively. The buckling criteria suggested that the free length shouldn't more than 0.42 m. So, the combination between wire diameter of 7 mm with coil diameter of 80 mm wasn't satisfied buckling criteria. Meanwhile, the combination between wire diameter of 8 mm and 9 mm with mean coil diameter of 80 mm were satisfied the buckling criteria. In addition, the free length of 0.875 m was obtained by using wire diameter of 7 mm and mean coil diameter of 100 mm. Meanwhile, the combination between wire diameter of 8 mm and 9 mm with mean coil diameter of 100 mm resulted in free length of 0.537 m and 0.383 m, respectively. The buckling criteria suggested that the free length shouldn't more than 0.526 m. So, the combination between wire diameter of 7 and 8 mm with coil diameter of 100 mm weren't satisfied the buckling criteria. Wire diameter of 7 mm wasn't satisfied the buckling criteria in the all range of mean coil diameter from 80 mm to 100. Meanwhile, wire diameter of 8 mm satisfied the buckling criteria only until mean coil diameter of 96 mm. The wire diameter of 9 mm satisfied the buckling criteria in the all range of mean coil diameter.

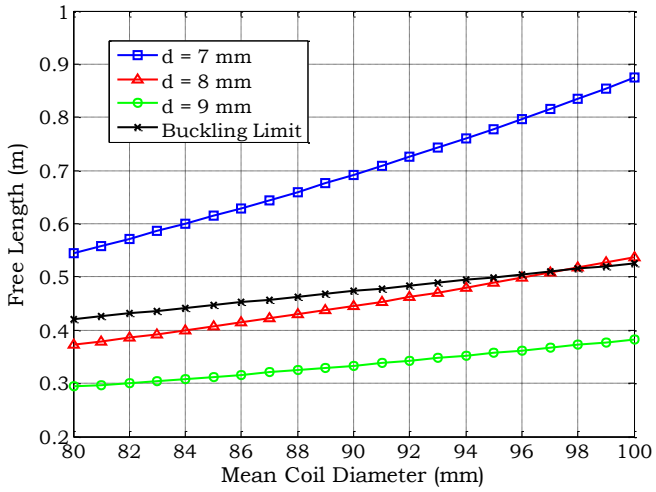

Figure 3-5: Mean Coil Diameter vs Free Length.

Figure 3-6 shows the relationship between mean coil diameter and energy storing. As shown in the figure, energy strong increased with increase in mean coil diameter. The energy storing of 103.6 N.m was obtained by using wire diameter of 7 mm and mean coil diameter of 80 mm. Meanwhile, the combination between wire diameter of 8 mm and 9 mm with mean coil diameter of 80 mm resulted in energy storing of 51.75 N.m and 28.09 N.m, respectively. In addition, energy storing of 202.4 N.m was obtained by using wire diameter of 7 mm and mean coil diameter of 100 mm. Meanwhile, the combination between wire diameter of 8 mm and 9 mm with mean coil diameter of 100 mm resulted in energy storing of 101.1 N.m and 54.87 N.m, respectively.

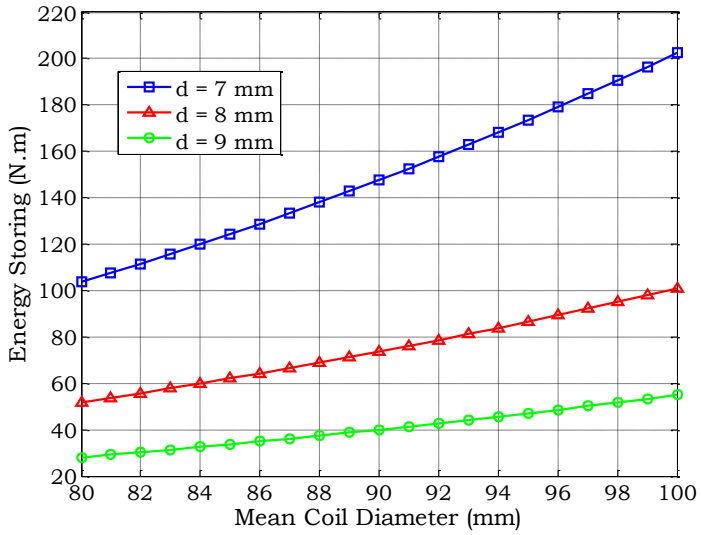

Figure 3-6: Mean Coil Diameter vs Energy Storing.

Figure 3-7 shows the relationship between mean coil diameter and separation velocity. The separation velocity of 1.86 m/s was obtained by using wire diameter of 7 mm and mean coil diameter of 80 mm. Meanwhile, the combination between wire diameter of 8 mm and 9 mm with mean coil diameter of 80 mm resulted in separation velocity of 1.31 m/s and 0.97 m/s, respectively. In addition, the separation velocity of 2.6 m/s was obtained by using wire diameter of 7 mm and mean coil diameter of 100 mm. Meanwhile, the combination between wire diameter of 8 mm and 9 mm with mean coil diameter of 100 mm resulted in separation velocity of 1.84 m/s and 1.35 m/s, respectively. Even, wire diameter of 7 mm, resulted the highest separation velocity, this wire diameter shouldn't be used due to buckling problem which may be occurred.

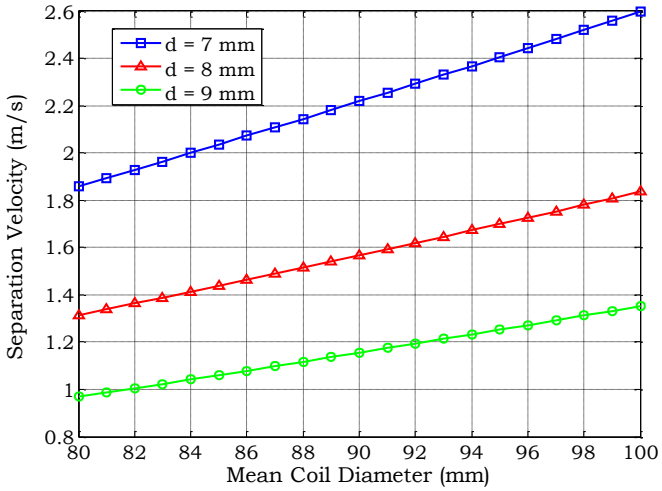

Figure 3-7: Mean Coil Diameter vs Separation Velocity.

4. Conclusions

Investigation of wire diameter of helical compression spring for payload separation has been conducted. The obtained result show that with payload weight of 60 kg, the minimum wire diameter should be 8 mm with mean coil diameter of 80 mm. In order to avoid buckling problem, for wire diameter of 8 mm, the maximum mean coil diameter which can be used was 96 mm. Wire diameter of 9 mm was free from buckling problem in the range of mean coil diameter of 80 – 100 mm. The maximum separation velocity of 1.76 m/s was obtained by using wire diameter of 8 mm and mean coil diameter of 96 mm.

Acknowledgements

Author wishes to thanks to Bambang Sapto Wibowo and Arief Budi Sanjaya for discussion about separation system. Authors also thanks to LAPAN for the support in publishing this research.

References

Abe, T., Nakamura, M., Ishii, N., & Inatani, Y. (2009). Recent Activities and Future Direction of Japanese Sounding Rocket Experiments for Scientific Purpose. *Proc. 19th ESA Symposium on European Rocket and Balloon Programmes and Related Research*, *2009*(September).

Budynas, R.G., Nisbett, J.K, & Shigley, J. E. (2008). *Shigley's Mechanical Engineering Design 8th Edition* (8th ed.). McGraw-Hill.

Chary, C. K., & Reddy, S. (2016). Design and Analysis of Helical Compression Spring of IC Engine. *International Advanced Research Journal in Science, Engineering and Technology*, *3*(10), 153–158. https://doi.org/10.17148/IARJSET.2016.31029

Hu, X., Chen, X., Tuo, Z., & Zhang, Q. (2012). Dynamics and transient perturbation analysis of satellite separation systems. *Proceedings of the Institution of Mechanical Engineers, Part G: Journal of Aerospace Engineering*, *227*(12), 1968–1976. https://doi.org/10.1177/0954410012466780

Hu, H., Wang, J., & Lu, W. (2008). Simulation and analysis of fairing jettison from sounding rocket. *Journal of Aeronautics, Astronautics and Aviation*, *40 A*(4), 237–244.

Inatani, Y., Ishii, N., Nonaka, S., & Abe, T. (2016). Recent Activities and Future Direction of Japanese Sounding Rocket Experiments for Scientific Purpose. *International Seminar on Aerospace Science and Technology IV*, 144–152.

Kolawole, S. O., Adewale, H., & Christian, O. (2018). Optimal Helical Spring Design for a P-Pod Using Chaotic Backtrack Search Algorithm. *International Journal of Scientific & Engineering Research*, *9*(8), 71–76. http://www.ijser.org

Li, J., Yan, S., & Tan, X. (2014). Dynamic-envelope analysis of clamp-band joint considering pyroshock of satellite separation. *Journal of Spacecraft and Rockets*, *51*(5), 1390–1400. https://doi.org/10.2514/1.A32382

Liu, Y., Li, Z., Sun, Q., Fan, X., & Wang, W. (2012). Separation dynamics of large-scale fairing section A fluid-structure interaction study.pdf. *Proceedings of the Institution of Mechanic Al Engineers Part G Journal of Aerospace Engineering*. https://doi.org/10.1177/0954410012462317

Pattar, S., Sanjay, S.J., & Math, V. . (2014). Static Analysis of Helical Compression Spring. *International Journal of Research in Engineering and Technology*, *03*(15), 835–838. https://doi.org/10.15623/ijret.2014.0315158

Samani, M., & Pourtakdoust, S. H. (2014). Analysis of Two - Stage Endo - Atmospheric Separation Using Statistical Methods. *Journal of Theoretical and Applied Mechanics*, *1992*, 1115–1124.

Sawanobori, T., Akiyama, Y., Tsukaharat, T., & Nakamura, M. (1985). Analysis of Static and Dynamic Stresses in Helical Spring. *Bulletin of Japan Society of Mechanical Engineers*, *28*, 725–734.

Tayefi, M., & Ebrahimi, M. (2009). Design and analysis of separation systems based on an optimization approach. *47th AIAA Aerospace Sciences Meeting Including the New Horizons Forum and Aerospace Exposition*, *January*, 1–10. https://doi.org/10.2514/6.2009-436